Observation of intermediate stages during light-induced halide segregation in wide bandgap halide perovskites

Finn Babbe, Eloïse Masquelier, Zhi Zheng, Carolin M. Sutter-Fella

Chemical Sciences Division, Joint Center for Artificial Photosynthesis, Lawrence Berkeley National Laboratory

Abstract:

Mixed halide perovskites sparked great research interest due to their outstanding optoelectronic properties, ease of fabrication and bandgap tunability. Within the ABX_3 structure, especially the composition of the X-site is varied to tune the bandgap, mostly using iodide and bromide. Those mixed perovskites however suffer from phase instabilities under illumination in which microscopic clusters with high iodide content are formed and act as recombination centers. The key mechanism(s) underlying this halide segregation process are still debated. We investigated the influence of microstructure and in particular, grain size and heterogeneity, on this process for the archetype perovskite $MAPb(I_{1.5}, Br_{1.5})$. Our findings show that the segregation process occurs in three stages (not two as commonly reported) and starts with a flash formation of I-rich nano domains. The composition of those nano domains depends on the grain size due to the prevalent compositional fluctuations as well as the abundance of defect states at grain boundaries.

Introduction

Their impressive opto-electronic properties and the comparably cheap processing have made halide perovskites promising candidates for a multitude of applications like photocatalytic devices, transistors, LEDs, and solar cells. Especially in the area of photovoltaics perovskites have shown the immense potential, reaching 25.2 % power conversion efficiency.[1]

However, in wide bandgap perovskites, halide segregation processes critically impacts the performance and durability of devices, limiting the viability of this technology.[2]

Team

Finn Babbe   Eloise Masquelier   Zhi Zheng   Carolin M. Sutter-Fella
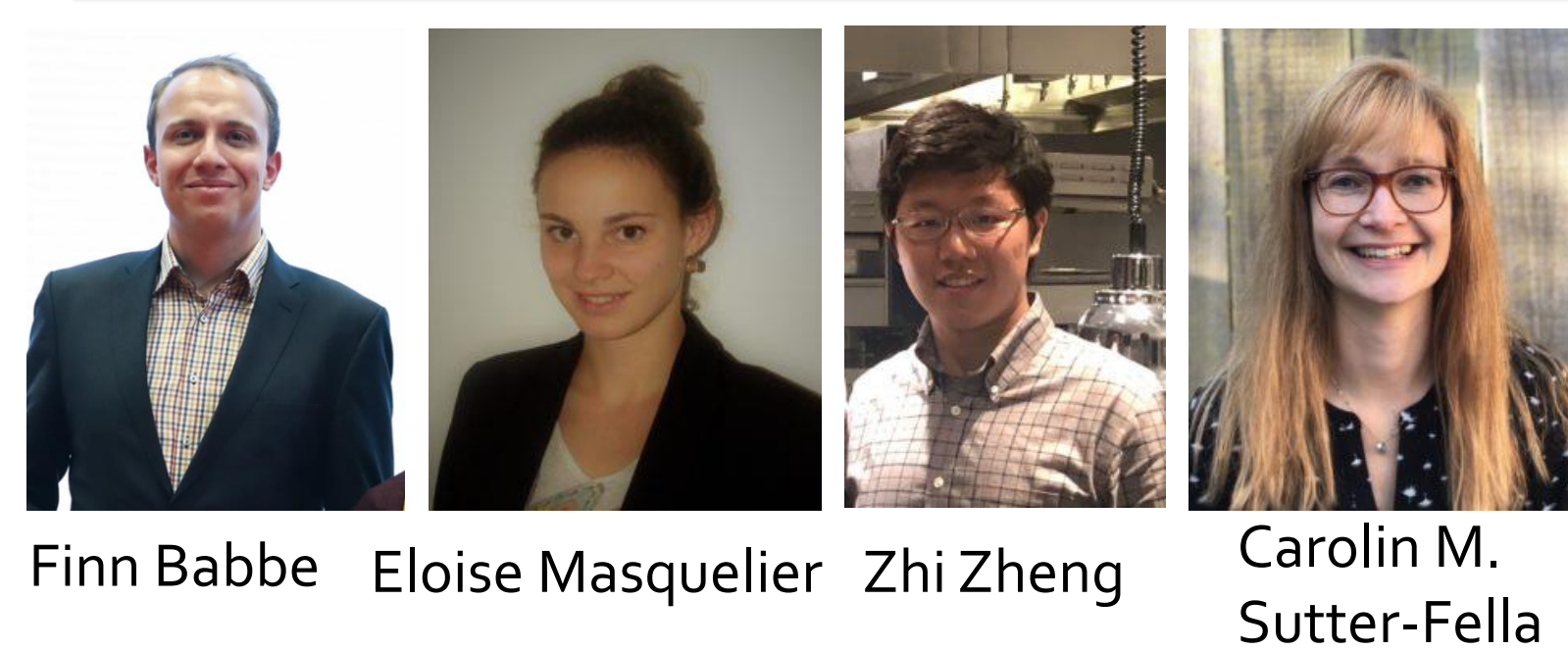
Broader Impact

Especially the easily tunable high bandgap makes halide perovskites attractive for direct photocatalysis and tandem solar cells.[3] To make those applications viable, a detailed understanding of the underlying segregation mechanism is needed to successfully prevent instabilities and avoid voltage losses. [4]

Our findings reveal a more complicated picture of the segregation mechanism proceeding in 3 instead of so far observed 2 stages. Likely due to the flash formation of iodide rich nano clusters. This understanding is important to stabilize halides in wide bandgap perovskites in future steps.

Acknowledgments

Results, Highlights, and Accomplishments

Halide perovskites

A — Organic and/or inorganic cations (MA, FA, Cs, Rb)
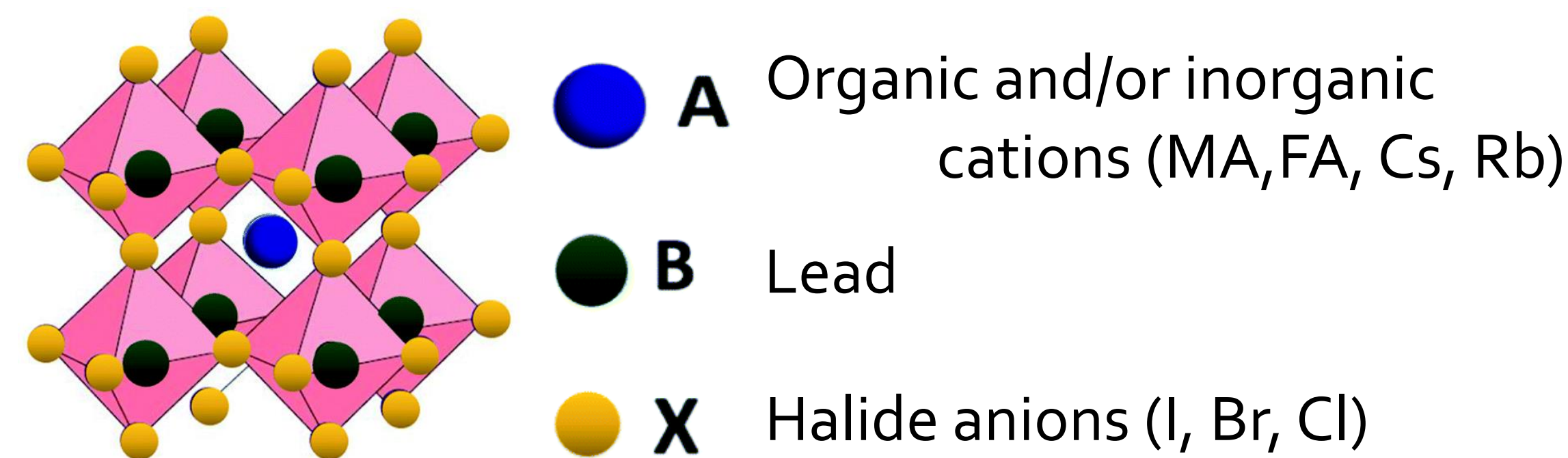B — Lead
X — Halide anions (I, Br, Cl)

Figure 1: Crystalline structure of perovskite (ABX_3) [5].

Tunable band gap via halide substitution, from 1.57 eV to 2.3 eV in $MAPb(I_{1-x}Br_x)_3$ perovskite film as x increases.

Applications: photocatalysis, H2 generation, CO2 reduction, color-tunable LEDs, photovoltaics and tandem solar cells.

Fabrication

Perovskites films are solution processed, presenting an easy and low-cost fabrication method. Films are spin-coated with the use of an antisolvent and an annealing step to enhance perovskite quality. By varying the annealing time between 30 seconds and 10 minutes the average grain size is varied between 80 nm and 150 nm.

precursor   antisolvent

100°C
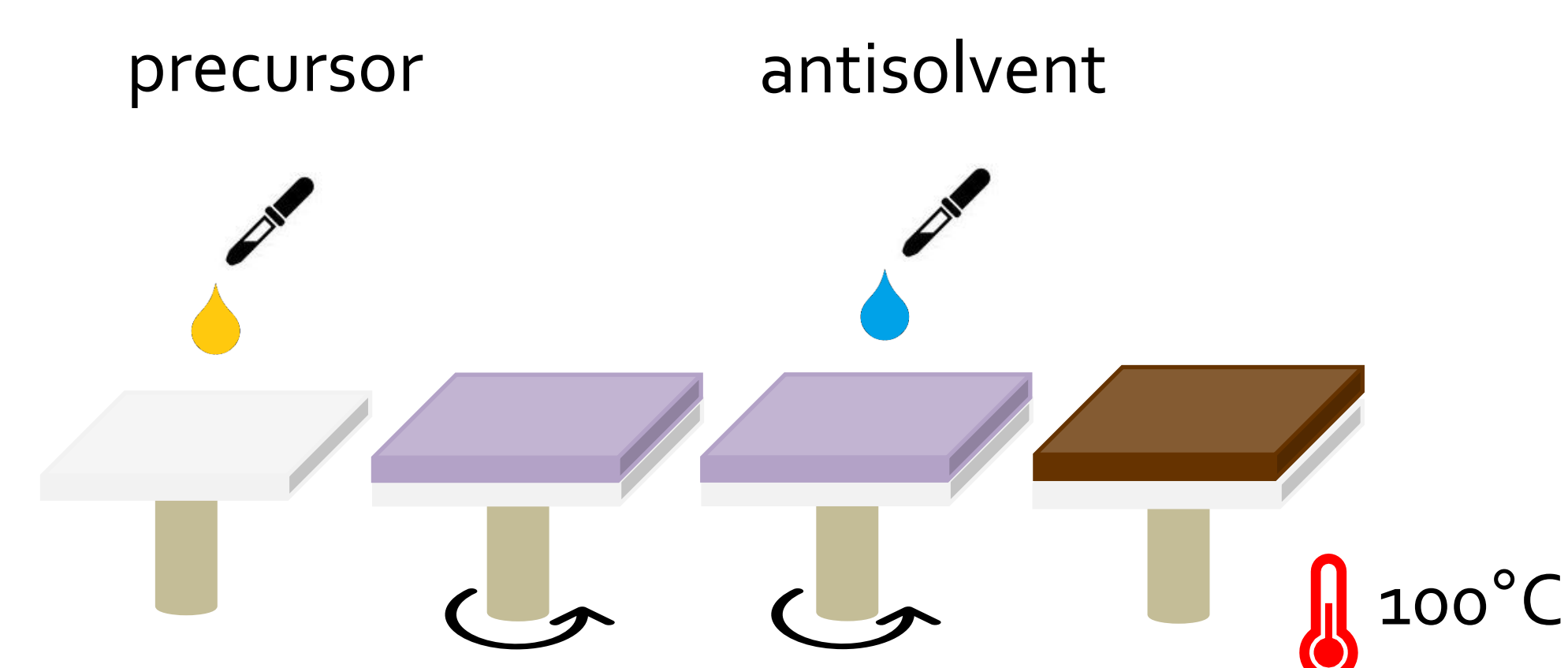
Characterization

XRD measurements are used to verify the composition and check for secondary phases. Sample morphology and grain size is characterized by SEM images. The investigated samples are phase pure and show no pinholes.
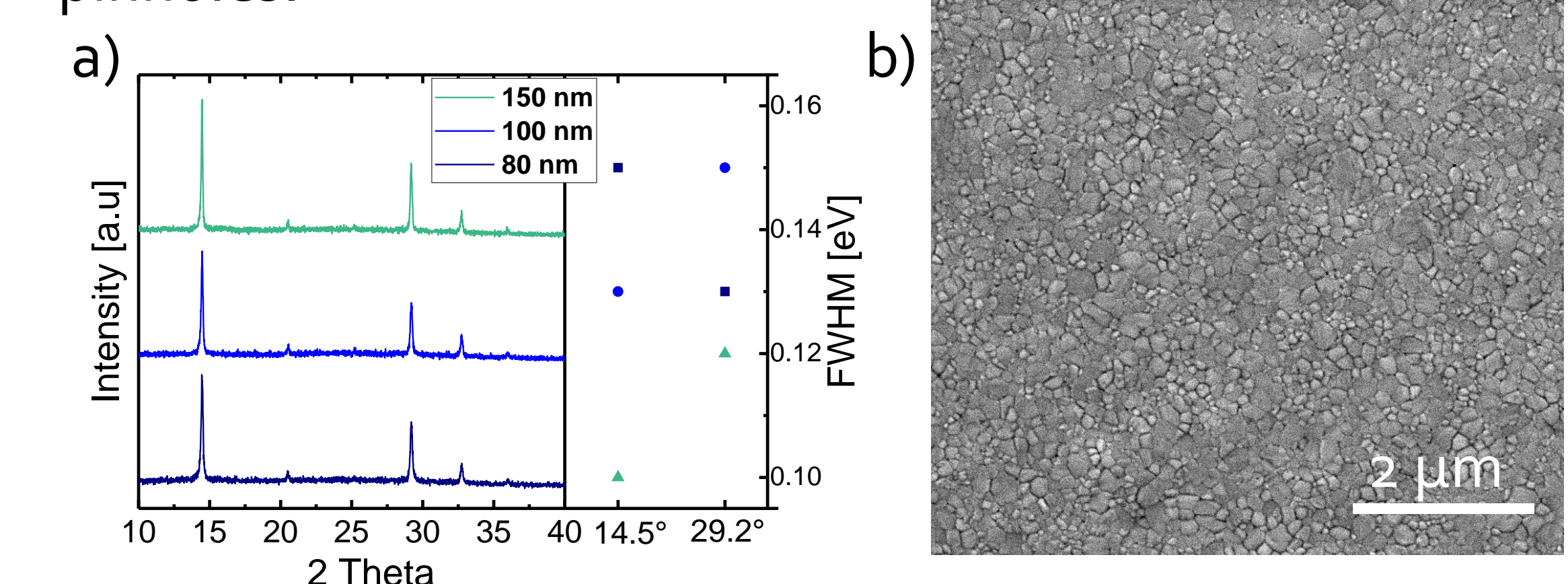
Figure 2: a) XRD patterns of $MAPb(I_{0.5}Br_{0.5})_3$ with varying grain size b) SEM image of $MAPb(I_{0.5}Br_{0.5})_3$ fabricated with a 10 minute annealing step.

Introduction de-mixing

Perovskites with mixed halides (I and Br) de-mix under illumination, giving rise to iodide rich clusters with a corresponding lower bandgap, resulting in a voltage loss. Commonly a low energy peak forms and shifts towards lower energies.
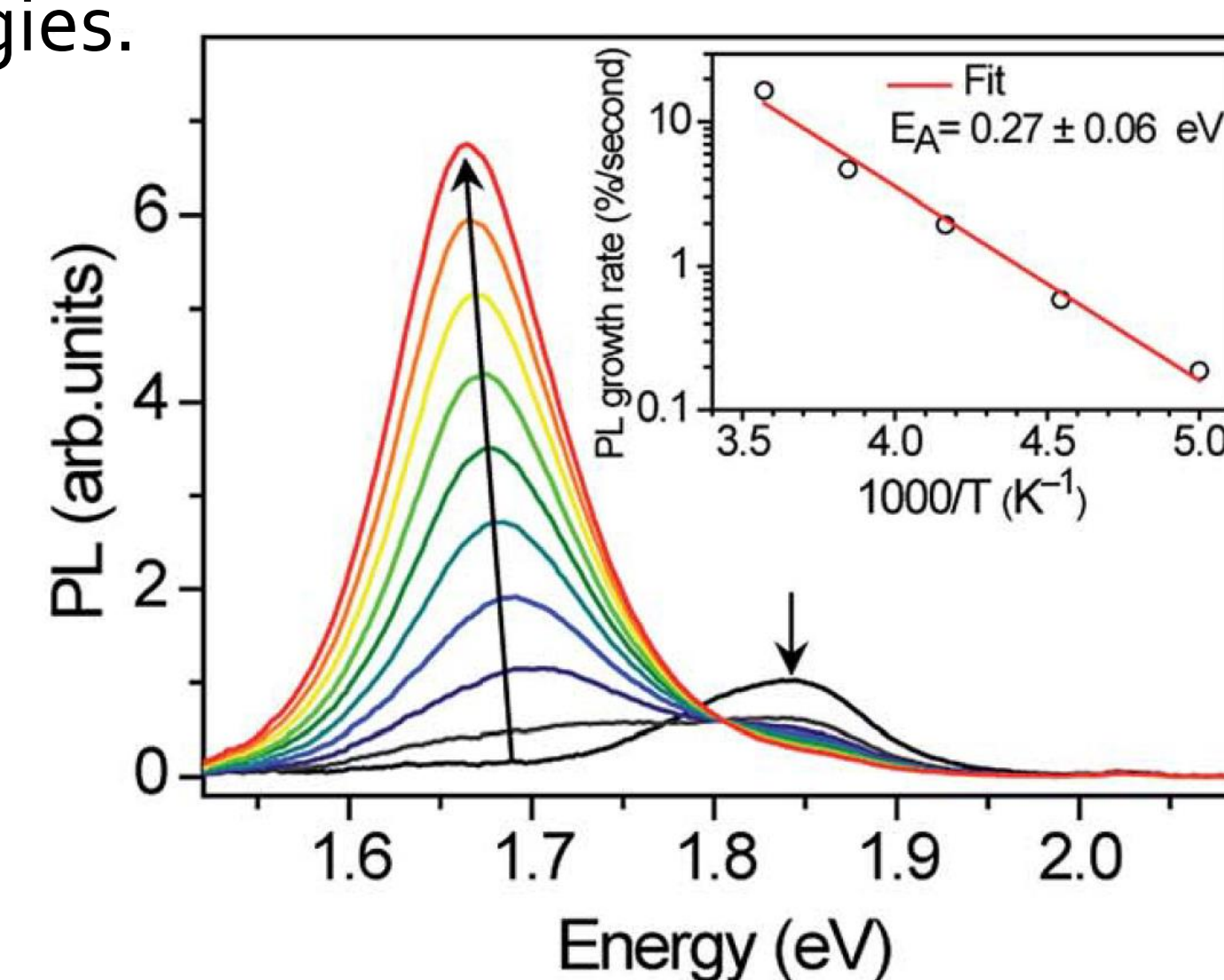

Figure 3: Photoluminescence (PL) spectra during halide segregation as reported in literature [6].

Halide segregation measured

Our measurements show that the peak evolution is more evolved, with an initial peak at low energies. This peak then broadens in width and shifts towards higher energies and not towards lower energies as reported in literature so far.
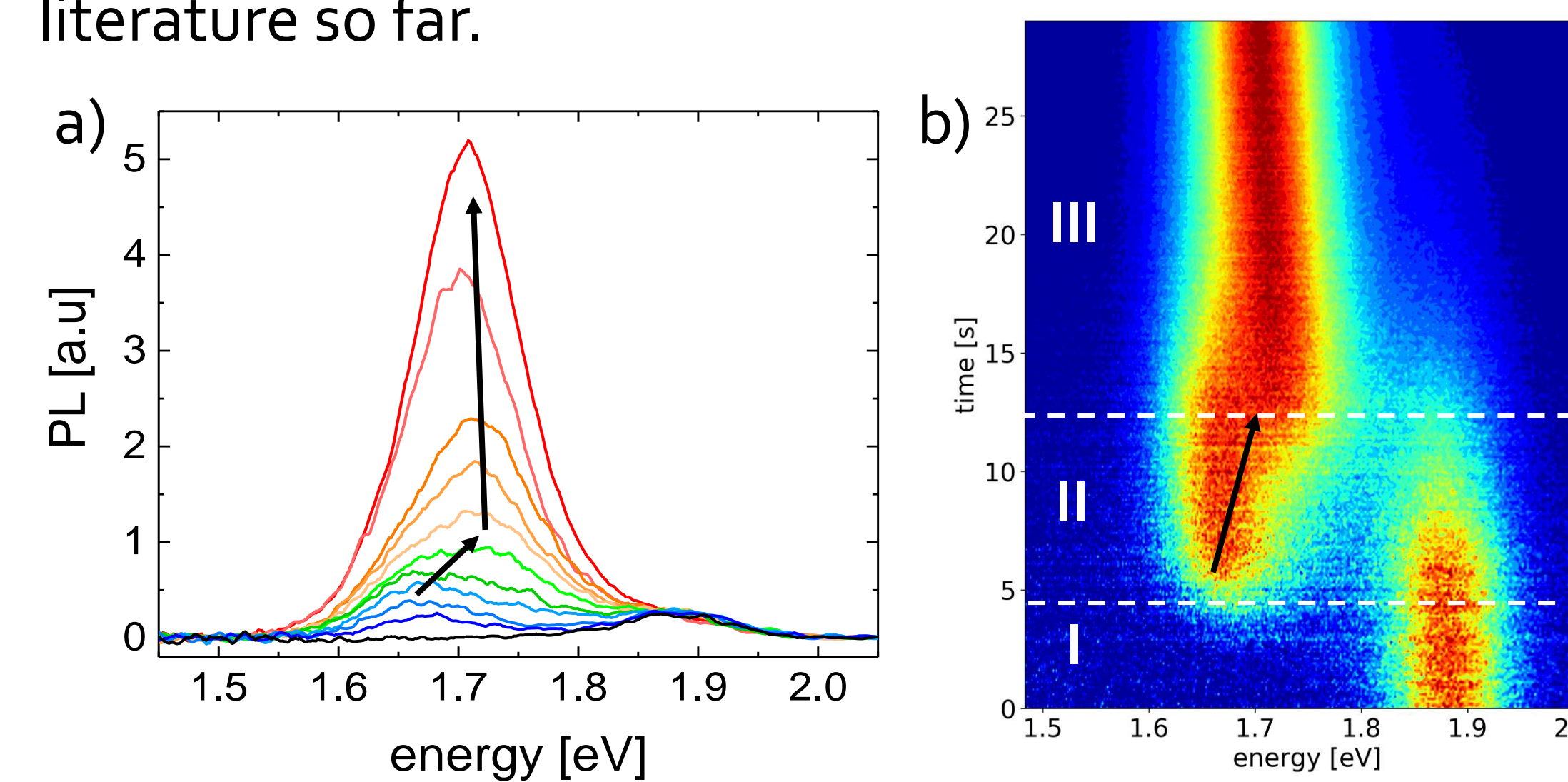
Figure 4: a) PL spectra and b) normalized contour plot of $MAPb(I_{1.5}Br_{1.5})$ under illumination revealing 3 distinct phases.

Trends with grain size

With decreasing grain size the initial peaks (E_0) and the final peak position (E_f) shift toward lower energies. Further the magnitude of the blue shift (ΔE) increases.
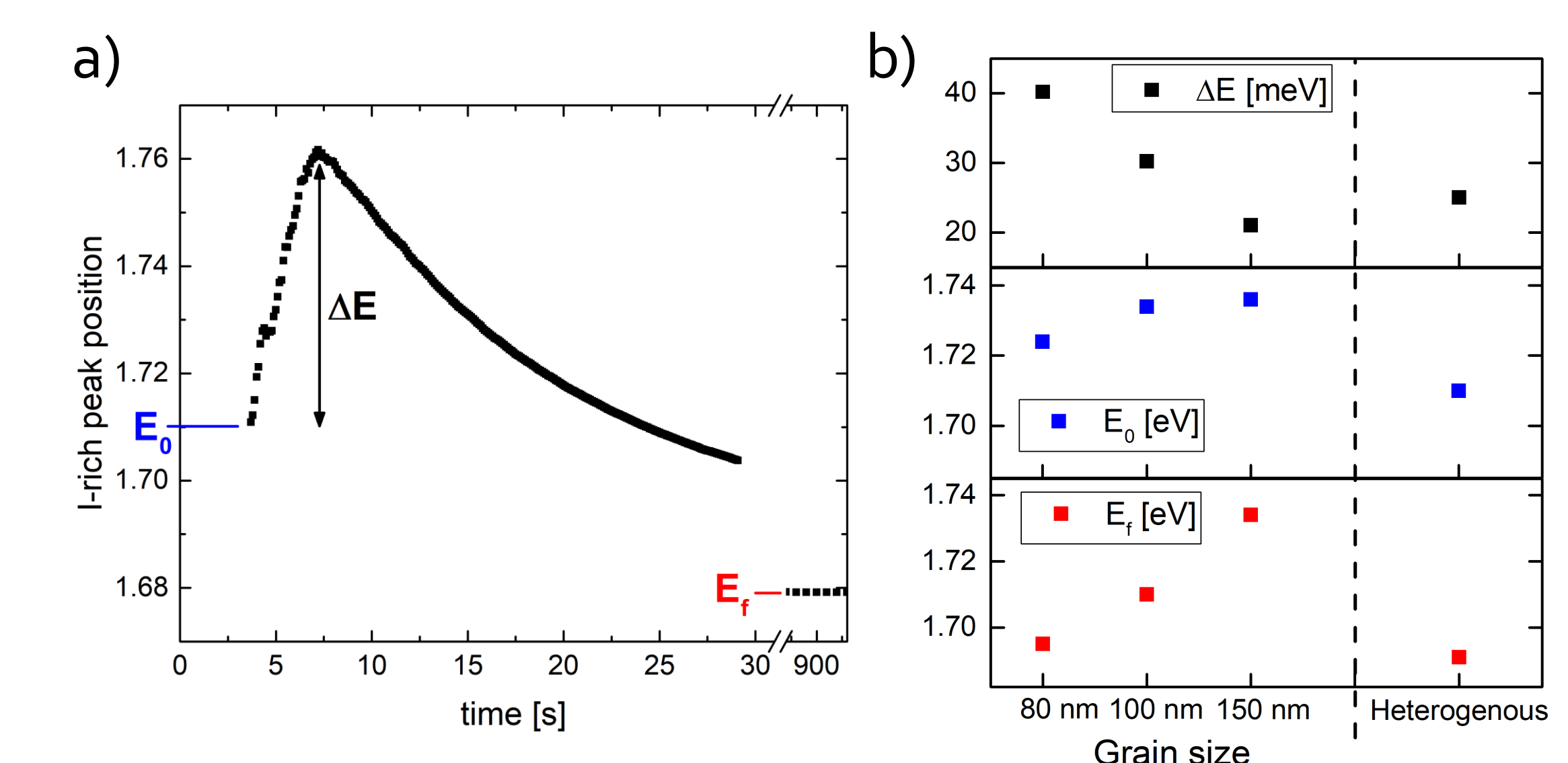
Figure 5: a) Evolution of the I-rich peak position over time and b) trends of key parameters of the degradation with grain size.

Reversibility and 50 °C

The segregation in three stages is fully reversible by leaving the sample in the dark for prolonged times.

Measurements at 50 °C show the same segregation process just with faster kinetics. No sign of degradation or loss of iodide is detected.
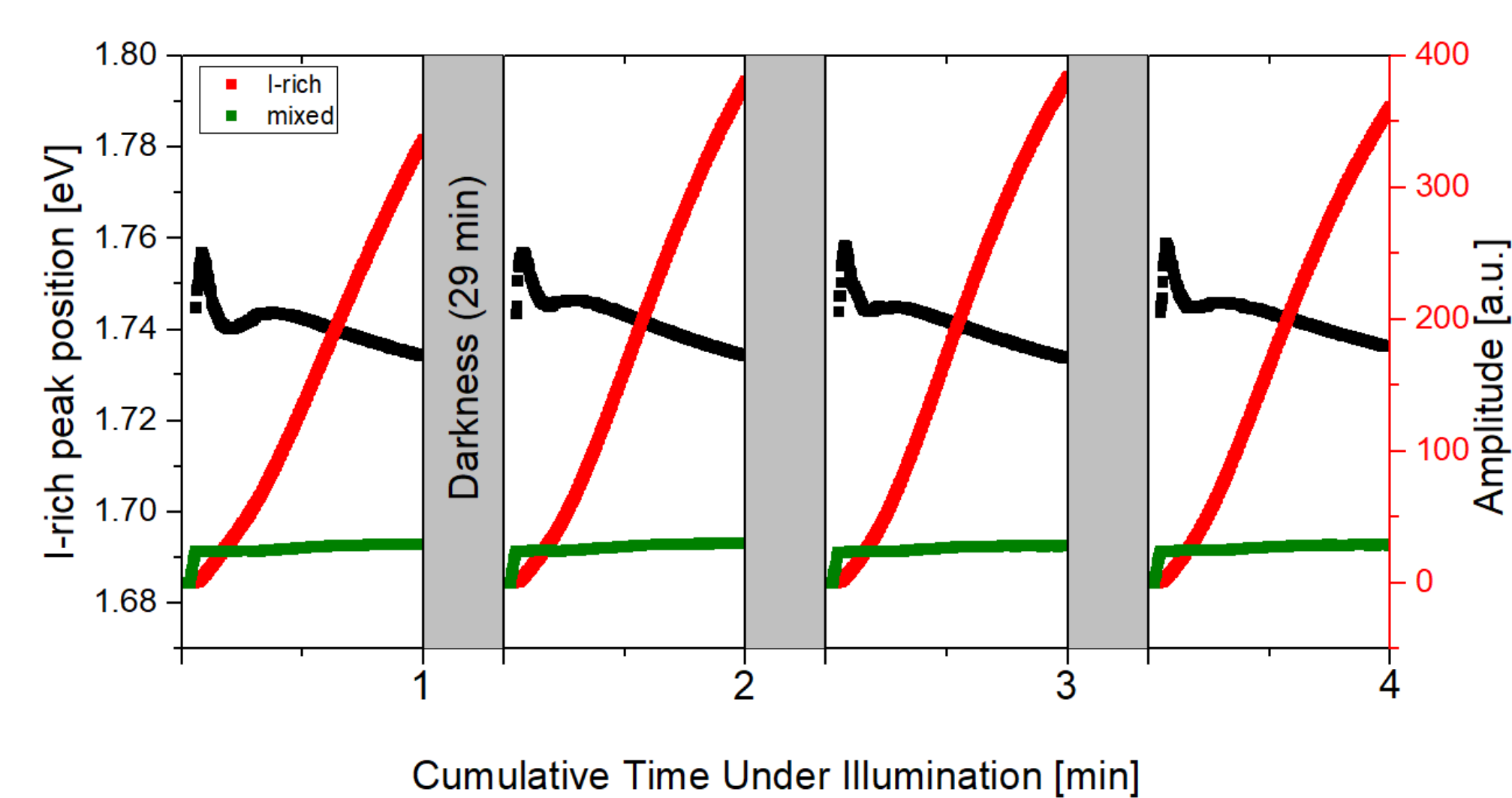

Figure 6: Peak position (black) and amplitude of the I-rich phase (red) and the mixed phase (green) during light/dark cycling.

Model for segregation

The blue shift is reversible and shows clear trends with grain size. We link the appearance of the initial low energy peak to the flash formation of iodide rich nano-clusters. Due to their low bandgap they channel most of the radiative recombination although they only make up a tiny fraction of the film. Over time clusters of various compositions form leading to a superposition of luminescence from all those clusters. This leads to a peak broadening as well as a blue shift, since the initial nano clusters don't dominate the PL emission anymore.
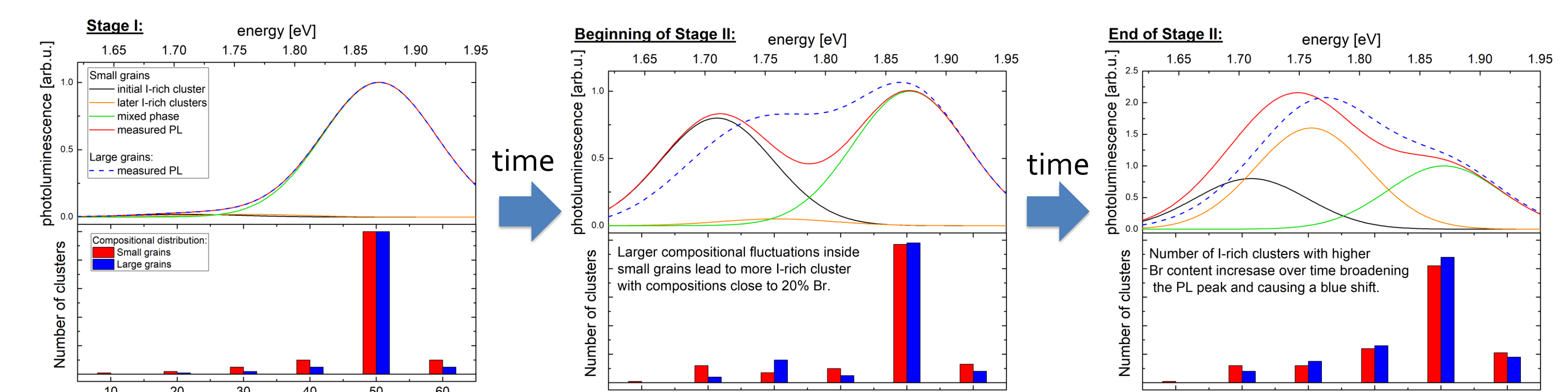
Literature

[1] NREL efficiency chart (link , visited 07/14/2020)
[2] Brennan, Trends in Chemistry, 2(4), 282–301, 2020.
[3] Huang et al., ACS Energy Letters, 5(4), 1107–1123, 2020
[4] Knight & Herz, Energy & Environ. Sci., 13(7), 2024–2046, 2020.
[5] Zijun Yi et al., Nanoscale Advances, 1(4), 1276–1289, 2019.
[6] Hoke et al., Chemical Science, 6(1), 613–617, 2015.